

Fluorometric sensing of Cu²⁺ ion with smart fluorescence light-up probe, triazolylpyrene (^{TNDMB}Py)

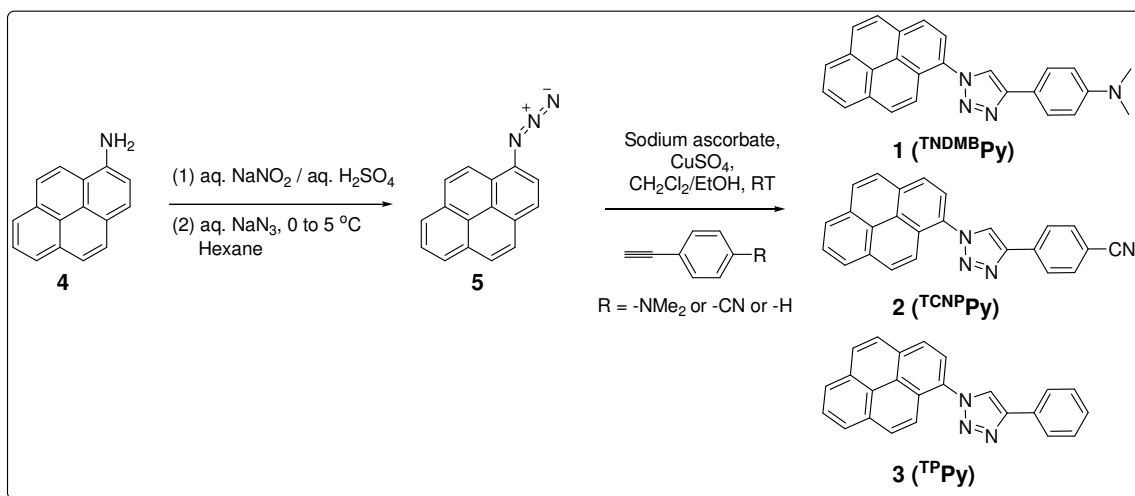
Subhendu Sekhar Bag,* Rajen Kundu and Sangita Talukdar

Bioorganic Chemistry Laboratory, Department of Chemistry, Indian Institute of Technology Guwahati, Guwahati-781039, Assam, India. Fax: +91-361-258-2349; Tel: +91-361-258-2324; E-mail: ssbag75@iitg.ernet.in

Contents	Page No.
1. Chemical synthesis	S2-S4
1.1. General Procedure for the Preparation of Aryl Azides	S2
1.2. General Procedure for the [3+2] Cycloaddition of Azides and Terminal Alkynes and the spectral data	S3-S4
2. Photophysical study	S4-S7
2.1. Emission spectra of 1 (^{TNDMB}Py) in different solvents.	S5
2.2. Emission spectra of 1 (^{TNDMB}Py) titrated with Cu²⁺ in CH₃CN.	S5
2.3. Fluorescence intensity change of 1 (^{TNDMB}Py) in presence of various metal ions	S6
2.4. Plot of intensity ratio of dual band titrated with Cu²⁺	S7
3. Job's plot of 1 (^{TNDMB}Py) with Cu²⁺ ion and the ESI-MS of 1.Cu²⁺ complex	S7-S8
4. Benesi-Hildebrand Plot	S8
5. Photophysical summary table of 1 (^{TNDMB}Py) titrated with Cu²⁺ ion	S9
6. Detection limit determination of 1 (^{TNDMB}Py) towards Cu²⁺ ion	S9
7. Cu²⁺ Selectivity in presence of various background interfering metal cations	S10
8. Fluorescence Studies in SDS Micelle Media	S10-S11
9. UV-Vis and emission spectra of 1 (^{TNDMB}Py) in presence of different metal ions	S11-S16
10. Comparison among the three fluorophores toward their efficiencies as selective fluorophores	S17
10.1. UV-Vis and emission spectra of fluorophores 2-3 in presence of different metal ions	S18-S21
10.2. Test for Selectivity in Sensing of Cu²⁺ Ion	S22-S23
11. Gaussian optimized geometry of 1.Cu²⁺ complex	S24-S26

1. Chemical synthesis

The fluorescent probes 1-3 were synthesized *via* our previously published method. Briefly, 1-aminopyrene (**4**) was converted to its corresponding 1-azidepyrene (**5**) *via* reaction with NaNO₂/aq. H₂SO₄ to diazonium salt followed by reaction with NaN₃ at 0 °C. Then, **5** react with terminal alkynes under click condition in presence of sodium ascorbate and CuSO₄ in a mixture of CH₂Cl₂-EtOH solvent at room temperature to form the product **1-3**.



Scheme S1: Synthesis of fluorescent probe **1** (**TNDMBPy**).

1.1. General Procedure for the Preparation of Aryl Azides

To an ice cold solution of sodium nitrite (3 eqv.) in water was added dropwise to a cold solution of aryl amine **1** (1 eqv.) in water and concentrated hydrochloric acid at 0 °C over 7 – 10 min. The reaction mixture was slowly stirred for 1 - 2 min before an ice cold solution of sodium azide (6 eqv.) in water was added dropwise at 0 °C over 10 min. The mixture was stirred for 15 min at 0 °C. The resulting mixture was extracted with ether. The organic layer was washed with water, followed by a brine solution, dried over anhydrous Na₂SO₄ and then concentrated to yield pure aryl azides. Formation of the product azide was confirmed from IR study (1-azidopyrene: Yield: 75%; IR: 2133 cm⁻¹) and the produced azide was then immediately used for the next step without further purification.

1.2. General Procedure for the [3+2] Cycloaddition of Azides and Terminal Alkynes and the spectral data

In a round bottom flask fitted with a septum, 1-azidopyrene (1.0 eqv.) was dissolved by dry 1:1 dichloromethane and ethanol and was degassed for 5 min with N₂. Then, alkyne (1.5 eqv.) was added and both the stirring and degassing were continued for next 5 min. After that a 6 mol % sodium ascorbate dissolved in water was added. The reaction mixture was stirred for 5 min and then 1 mol % powdered CuSO₄ dissolved in water was added. Degassing was continued for next 10 min. The reaction was allowed to proceed to room temperature and monitored by TLC. After total consumption of the starting azide, the reaction mixture was evaporated completely to a solid material and partitioned between water and ethyl acetate. The organic layer was washed with water followed by brine solution, dried over Na₂SO₄ and then concentrated. The title triazolyl-compounds were separated by column chromatography and characterized.

Synthesis of N, N-dimethyl-4-(1-(pyren-1-yl)-1H-1,2,3-triazol-4-yl)benzenamine (1): Using the general procedure, starting from 0.025 g of 1-azidopyrene (**5**) and 0.022 g of 4-*N,N*-dimethylaminophenylacetylene, 0.024 g of the title compound **1** was isolated as a light pink solid (68% yield). IR (KBr): 1617, 1567, 1503, 1460, 1351, 819 cm⁻¹; ¹H NMR (CDCl₃; 400 MHz) δ 3.03 (6H, s), 6.84 (2H, d, *J* = 8.0 Hz), 7.87 (2H, d, *J* = 8.4 Hz), 7.97 (1H, d, *J* = 9.2 Hz), 8.06 – 8.20 (6H, m), 8.24 – 8.29 (3H, m); ¹³C NMR (CDCl₃; 100 MHz) δ 40.6, 112.7, 118.6, 121.4, 123.5, 124.3, 124.9, 125.2, 126.1, 126.5, 126.9, 127.1, 128.9, 129.7, 130.8, 131.3, 132.3, 148.6, 150.8; HRMS calcd. for C₂₆H₂₁N₄ ([M+H]⁺) 389.1766, found 389.1768.

Synthesis of 4-(1-(pyren-1-yl)-1H-1,2,3-triazol-4-yl)benzotrile (2): Using the general procedure, starting from 0.09g of 1-azidopyrene (**5**) and 0.071 g of 4-ethynylbenzotrile, 0.068 g of the title compound **2** was isolated as a red solid (50% yield). IR (KBr): 2222, 1613, 1489, 1459, 848 cm⁻¹; ¹H NMR (CDCl₃; 400MHz) δ 7.77 (2H, d, *J* = 8.0 Hz), 7.88 (1H, d, *J* = 8.8 Hz), 8.08 – 8.20 (6H, m), 8.23 – 8.32 (4H, m), 8.36 (1H, s); ¹³C NMR (CDCl₃; 100 MHz) δ 112.0, 118.9, 121.0, 123.5, 124.0, 124.3,

124.9, 125.3, 126.5, 126.9, 127.1, 129.4, 130.2, 130.8, 131.3, 132.7, 133.1, 134.9, 146.3; ESI-TOF-MS m/z 371 $[M+H]^+$; HRMS calcd. for $C_{25}H_{15}N_4$ ($[M+H]^+$) 371.1297, found 371.1302.

Synthesis of 1-(Pyren-1-yl)-1H-1,2,3-triazol-4-yl-benzene (3): Using the general procedure, starting from 0.1 g of 1-azidopyrene (**5**) and 0.063 g of 1-phenylacetylene, 0.085 g of the title compound **3** was isolated as a white solid (60% yield). IR (KBr): 1510, 1461, 1037, 836.8 cm^{-1} ; 1H NMR ($CDCl_3$, 400MHz) δ 7.40 (1H, t, $J = 7.6$ Hz), 7.50 (2H, t, $J = 7.6$ Hz), 7.93 (1H, d, $J = 8.8$ Hz), 8.00 (1H, d, $J = 7.2$ Hz), 8.06 – 8.24 (7H, m), 8.27 (1H, s), 8.29 (1H, s); ^{13}C NMR ($CDCl_3$, 100 MHz) δ 121.3, 122.9, 123.5, 124.3, 124.9, 125.2, 126.1, 126.3, 126.4, 126.6, 126.9, 127., 128.6, 129.2, 129.9, 130.6, 130.9, 131.3, 132.5, 148.1; ESI-TOF-MS m/z 346 $[M+H]^+$.

2. Photophysical study

All the UV –visible spectra of the compounds (10 μM) in presence of various metal ions with different concentration were measured using a UV-Visible spectrophotometer with a cell of 1 cm path length.

All the sample solutions were prepared as described in UV measurement experiments. Fluorescence spectra were obtained using a fluorescence spectrophotometer at 25 $^{\circ}C$ using 1 cm path length cell. The fluorescence quantum yields (Φ_f) were determined using quinine sulphate as a reference with the known Φ_f (0.54) in 0.1 molar solution in sulphuric acid.

2.1. Emission spectra of **1** (^{TNDMB}Py) in different solvents.

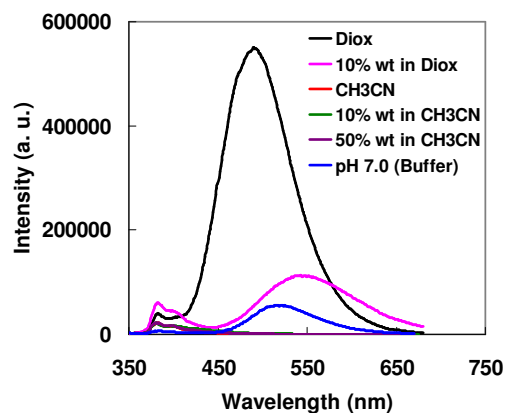


Figure S1: Emission spectra of **1** (^{TNDMB}Py) in different solvents.

2.2. Emission spectra of **1** (^{TNDMB}Py) titrated with Cu²⁺ ion

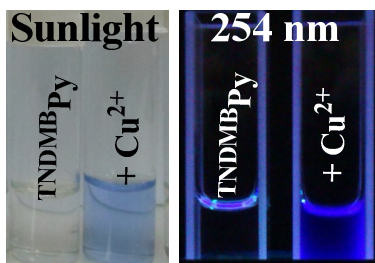
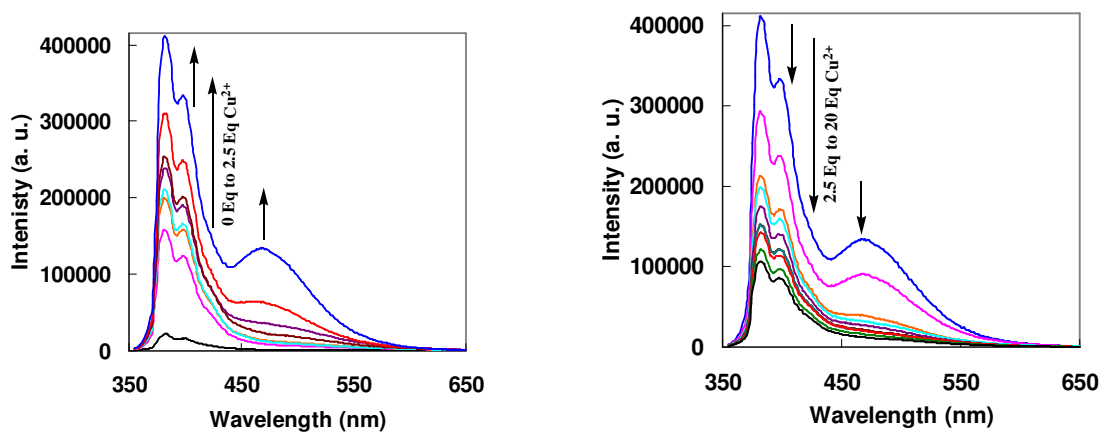


Figure S2. Emission spectra of **1** (^{TNDMB}Py) titrated with Cu²⁺ ion and the colour change indicating the complexation *via* N-coordination in day light and the emission image under transilluminator (254 nm).

2.3. Fluorescence intensity change of **1** (^{TNDMB}Py) in presence of various metal ions

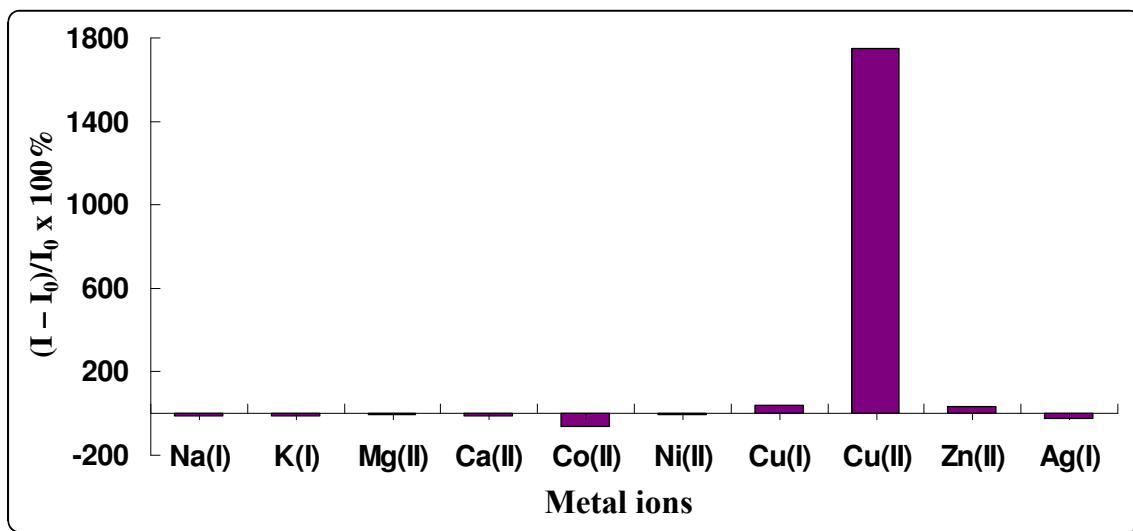
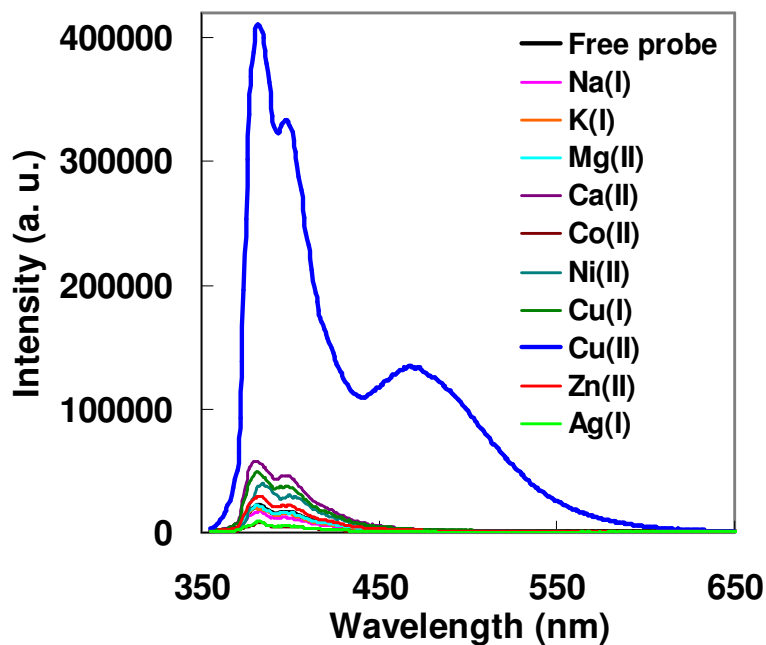


Figure S3: Fluorescence intensity changes $((I - I_0)/I_0 \times 100\%)$ of **1** (^{TNDMB}Py) (10 μ M) at 298 K upon addition of various metal ions (2.5 equiv). Excitation wavelength was at 343 nm. I_0 is fluorescent emission intensity at 383 nm of free host and I is the fluorescence intensity after adding metal ions.

2.4. Plot of intensity ratio of dual band titrated with Cu^{2+}

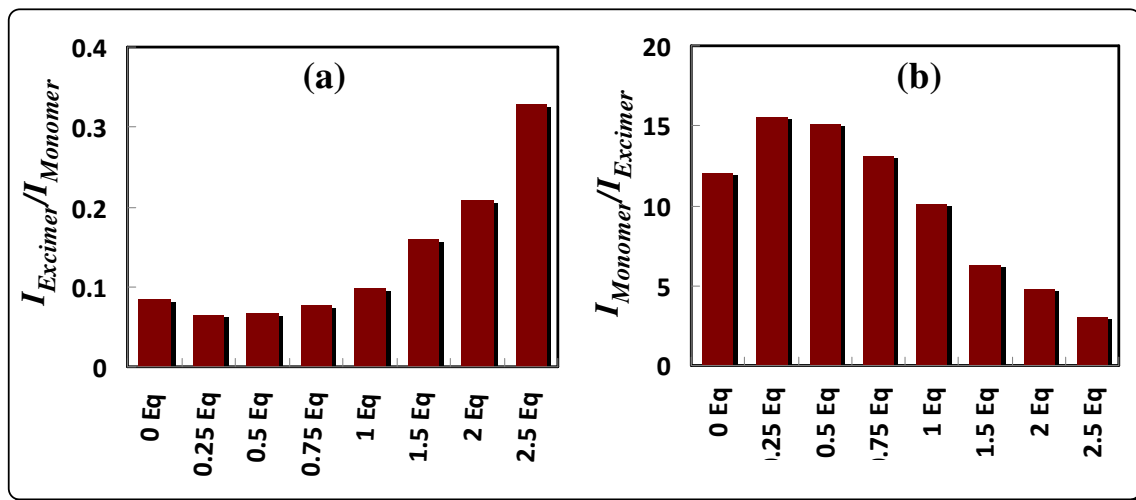


Figure S4: Plot of I_{Excimer} to I_{Monomer} (a) and I_{Monomer} to I_{Excimer} (b) ratio of 1 (TNDMBPy) titrated with Cu^{2+} in CH_3CN

3. Job's plot of 1 (TNDMBPy) with Cu^{2+} ion and the ESI-MS of 1. Cu^{2+} complex

Job's plot showed the 2:1 ligand-to-metal complexation which is also supported by an ESI-MS mass peak at m/z $[(\text{TNDMBPy})_2\text{Cu}-2\text{H}]^+$ 841.65.

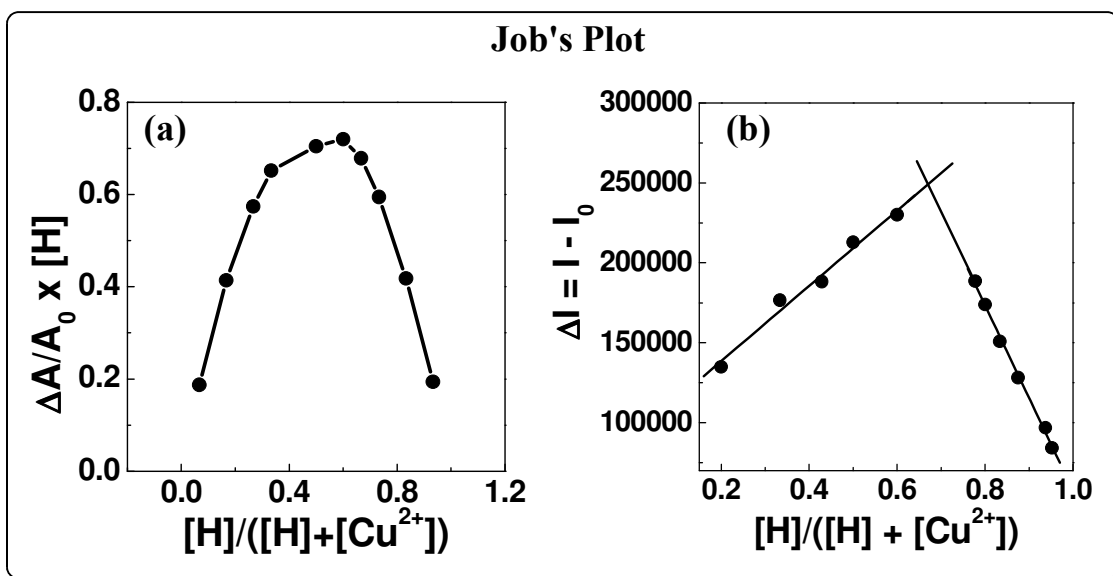


Figure S5: (a) Absorption and (b) fluorescence Job's plot of 1 (TNDMBPy) in presence of Cu^{2+} ion.

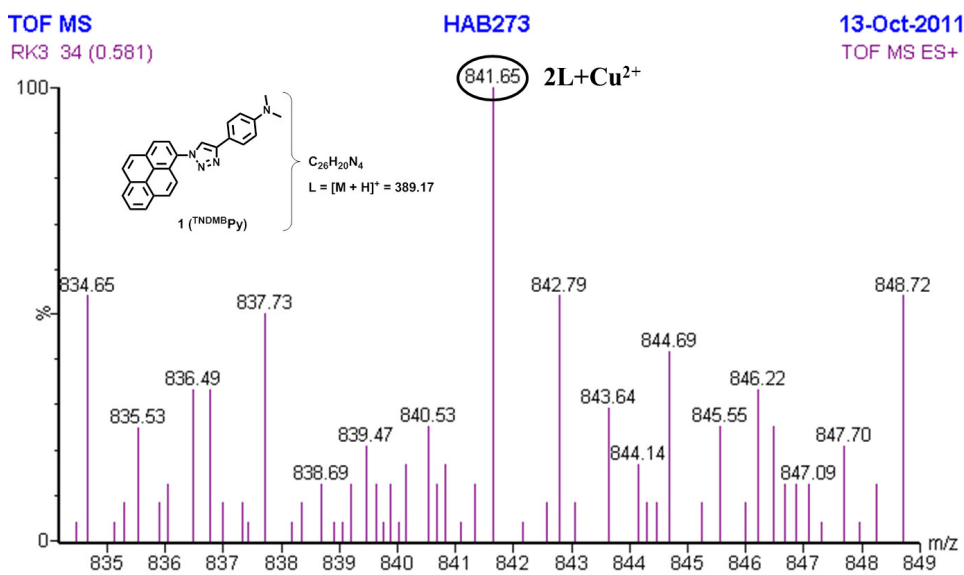


Figure S6: The ESI-MS of 2:1 ligand-to-metal complex of $[(^{TNDMB}Py)_2Cu-2H]^+$.

4. Benesi-Hildebrand Plot

The association constant of Cu^{2+} with $1 (^{TNDMB}Py)$ was determined by Benesi-Hildebrand plot using the following equation, which come as $2.23 \times 10^5 M^{-1}$.

$$\frac{1}{(I - I_0)} = \frac{1}{(I_\infty - I_0)} + \frac{1}{(I_\infty - I_0)K[Cu^{2+}]}$$

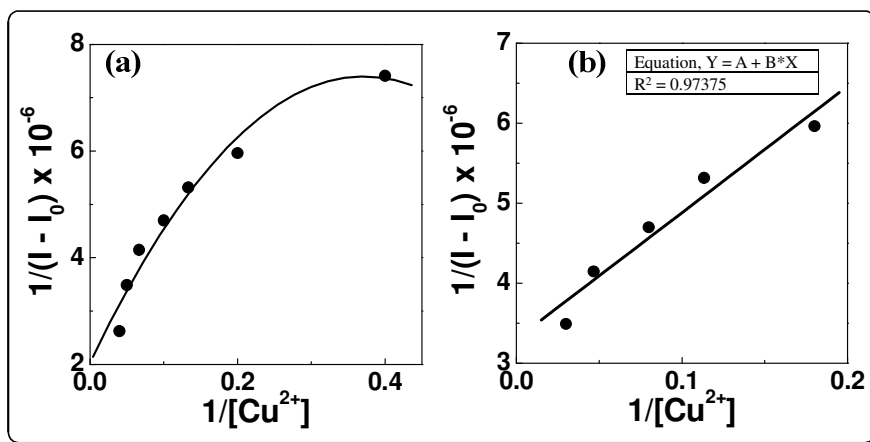


Figure S7: Benesi-Hildebrand plot of the monomer band of $1 (^{TNDMB}Py)$ with Cu^{2+} , (a) full region, (b) linear region.

5. Photophysical summary table of **1** (^{TNDMB}Py) titrated with Cu²⁺ ion

Table S1: Absorption, emission and quantum yield summary of **1** (^{TNDMB}Py) titrated with Cu²⁺ in CH₃CN

Cu ²⁺ (eqv.)	λ_{\max}^{abs}	Abs	$\lambda_{mono}^{fl} / \lambda_{exci}^{fl}$	Φ_f
0.00	276/343	0.287/0.191	382	0.003
0.25	276/343	0.286/0.194	382	0.020
0.50	276/343	0.286/0.197	382	0.026
0.75	276/343	0.279/0.193	382	0.026
1.00	276/343	0.276/0.195	382/466	0.035
1.50	276/343	0.267/0.197	382/466	0.038
2.00	276/343	0.267/0.202	382/466	0.049
2.50	276/343	0.281/0.208	382/466	0.073

6. Detection limit determination of **1** (^{TNDMB}Py) towards Cu²⁺ ion

We have calculated the detection limit of the fluorescent probe **1** towards Cu²⁺ ion by plotting $(I_{min} - I)/(I_{min} - I_{max})$ vs. $\log[Cu^{2+}]$. The linear fit was drawn by taking the five points (2.5 μ M to 15 μ M) of the linear region. The extended line where it crossed the ordinate axis is the detection limit which comes in the region of 177 nM.

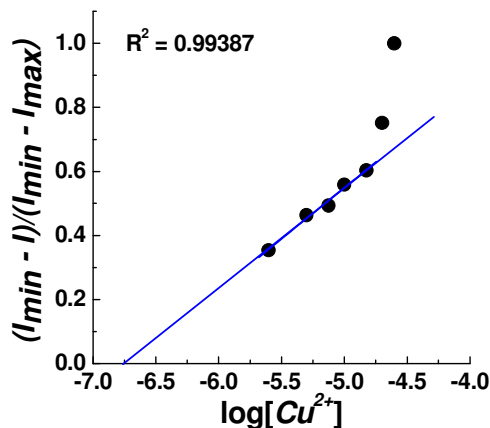


Figure S8: Plot of $(I_{min} - I)/(I_{min} - I_{max})$ vs. $\log[Cu^{2+}]$ of **1** for monomer band.

7. Cu²⁺ Selectivity in presence of various background interfering metal cations

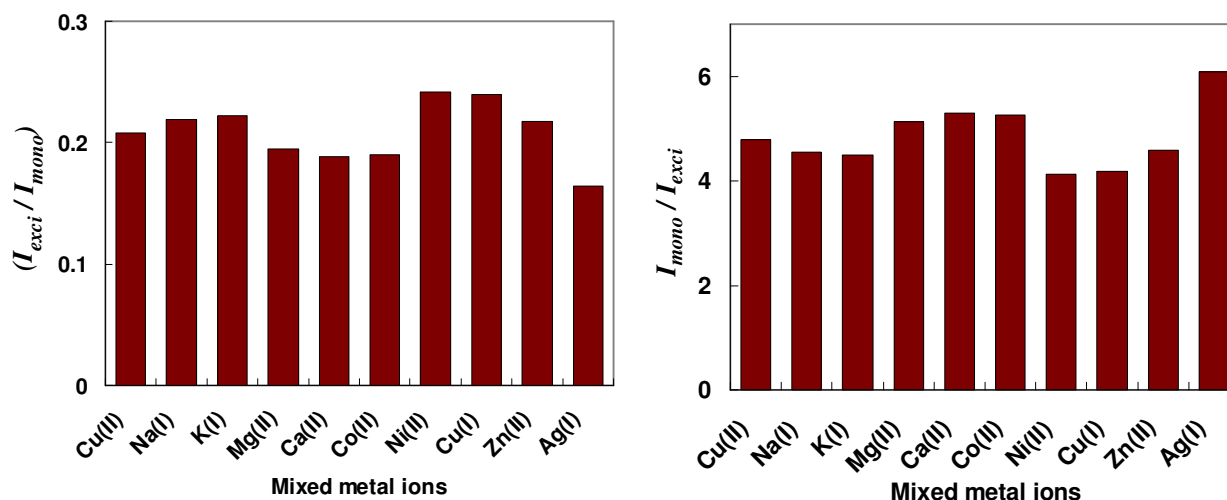


Figure S9: Ratio of fluorescence intensity at 466 and 384 nm of **1** (10 μ M) with Cu²⁺ (2.0 equiv.) in the absence and presence of different interfering metal ions (50 equiv.).

8. Fluorescence Studies in SDS Micelle Media

Surfactant (SDS) solution was prepared in MQ water. The concentration of SDS was 10 mM, above micellar concentration to make sure the formation of micelle in the experimental conditions. pH of the solutions was adjusted by dilute HCl and or dilute NaOH. The probe's solutions in SDS surfactant (10 mM) were mixed well and then Cu²⁺ ion (solution of [Cu(ClO₄)₂·6H₂O] in MQ water) of different concentrations were added maintaining the final volume 3 mL of the mixtures (10 μ M probe in 10 mM SDS solution and 0, 10, 25, 50, 75, 100, 125 *etc.* μ M Cu²⁺ ions respectively). Then again the whole solutions were mixed well before taking the fluorescence spectra. All the experiments were carried out at 25 °C.

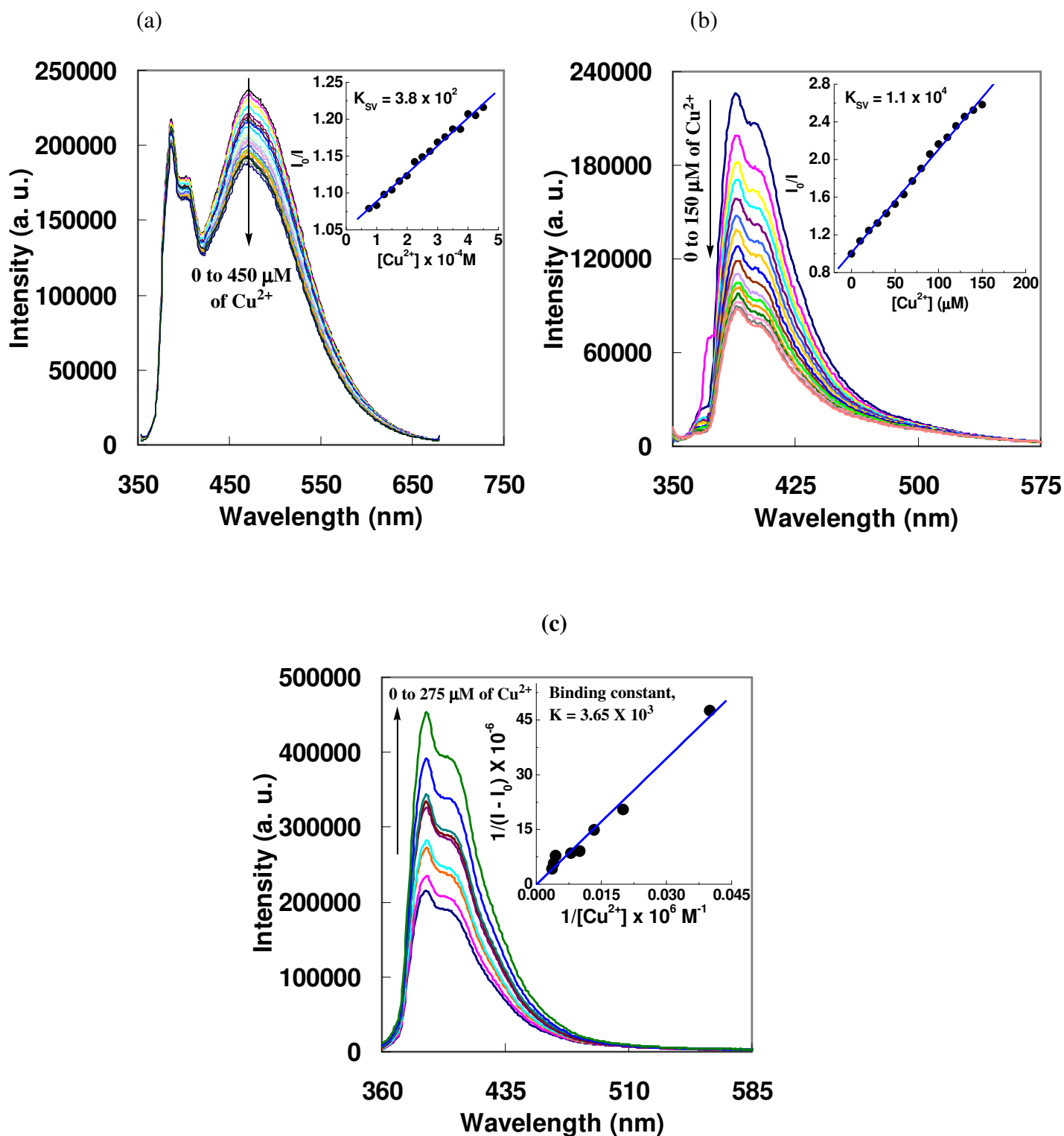


Figure 10: Emission behavior of triazolyl pyrene (10 μM) in presence of increasing concentration of Cu²⁺ ion in SDS micelle at (a) pH 2.0, (b) pH 7.0, and at (b) pH 8.0.

9. UV-Vis and emission spectra of **1** (^{TNDMB}Py) in presence of different metal ions

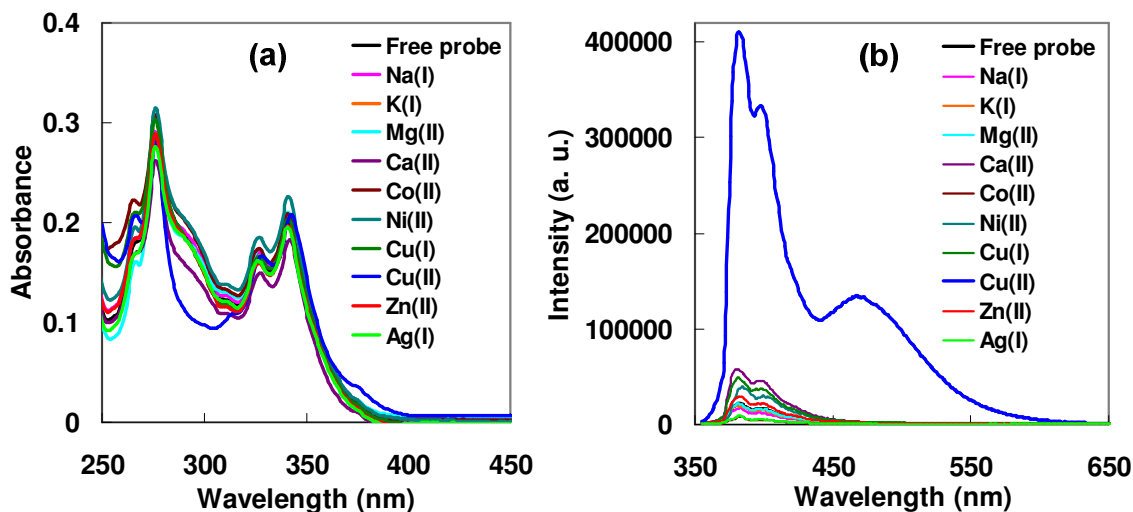


Figure S11: (a) UV-Vis, (b) Emission spectra of **1** (^{TNDMB}Py) (10 μM) in presence of various metal ions (2.5 equiv.).

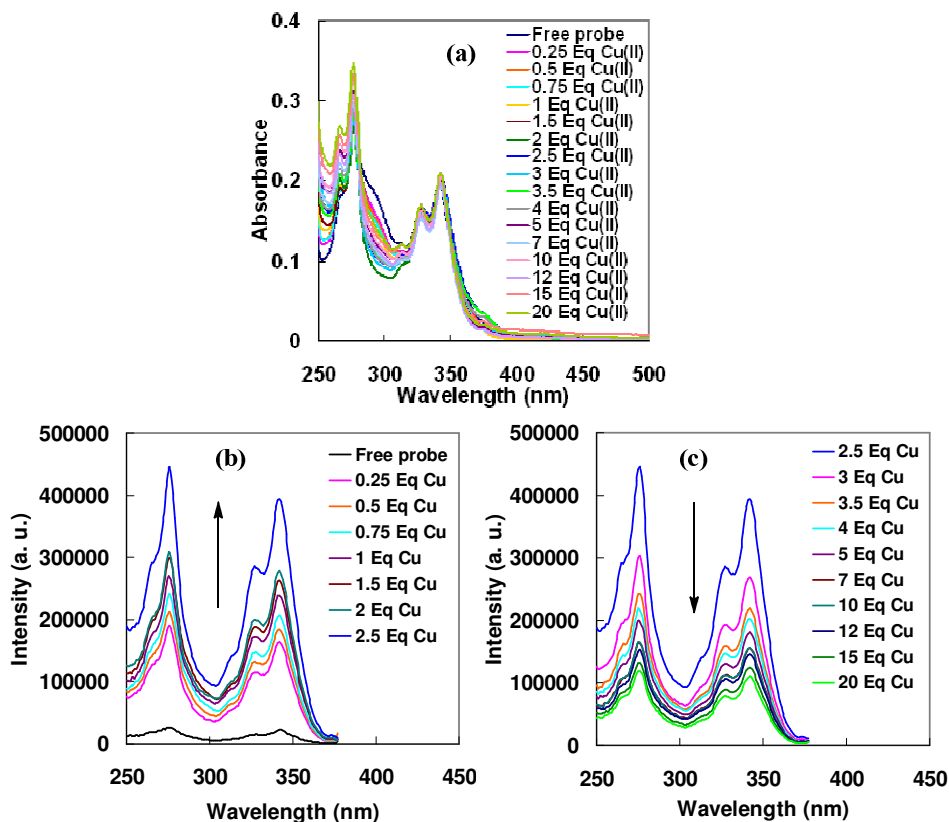


Figure S12: (a) UV-Vis, (b-c) excitation spectra of **1** (10 μM) in presence of Cu²⁺ ion.

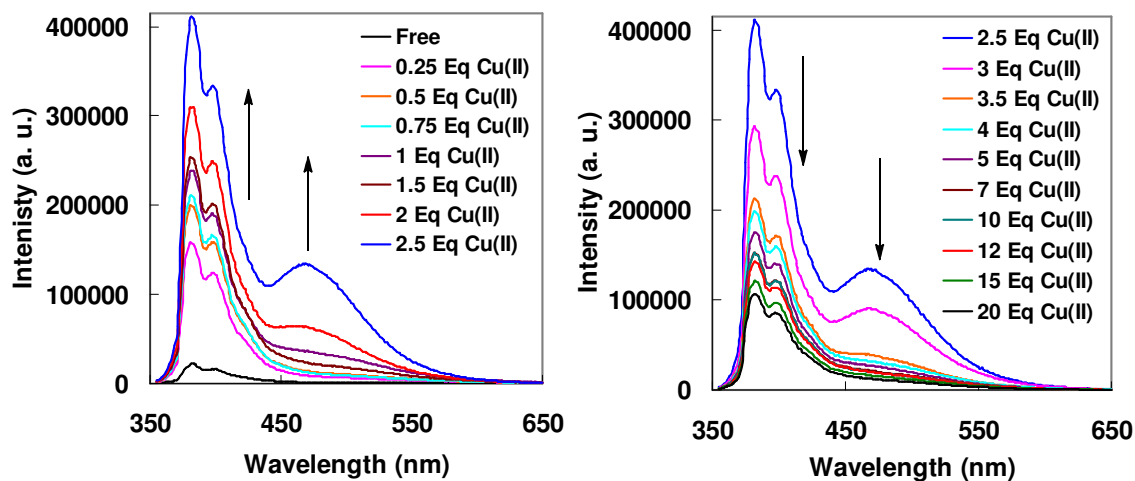


Figure S13: Emission spectra of **1** (10 μ M) in presence of Cu²⁺ ion in CH₃CN.

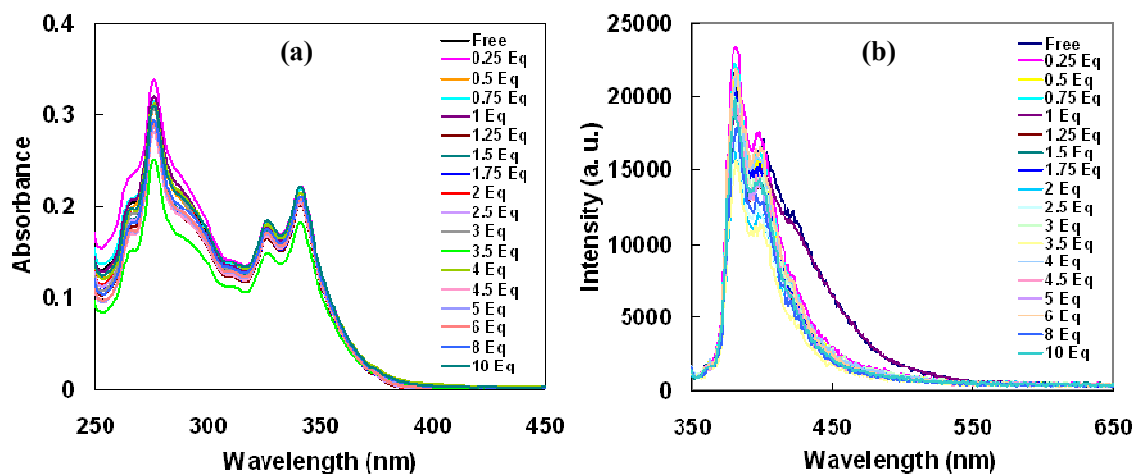


Figure S14: (a) UV-Vis, (b) emission spectra of **1** (10 μ M) in presence of Na⁺ ion.

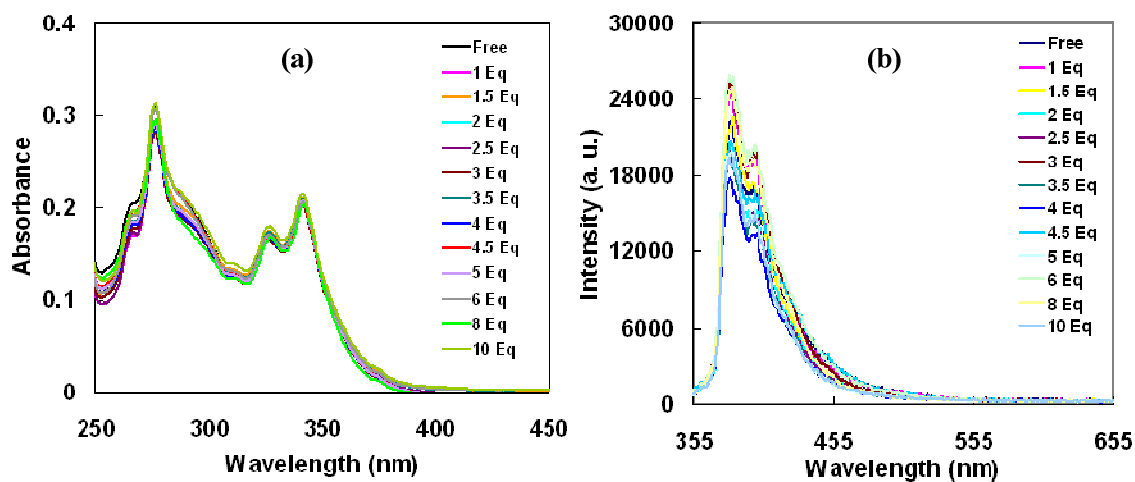


Figure S15: (a) UV-Vis, (b) emission spectra of **1** (10 μ M) in presence of K⁺ ion.

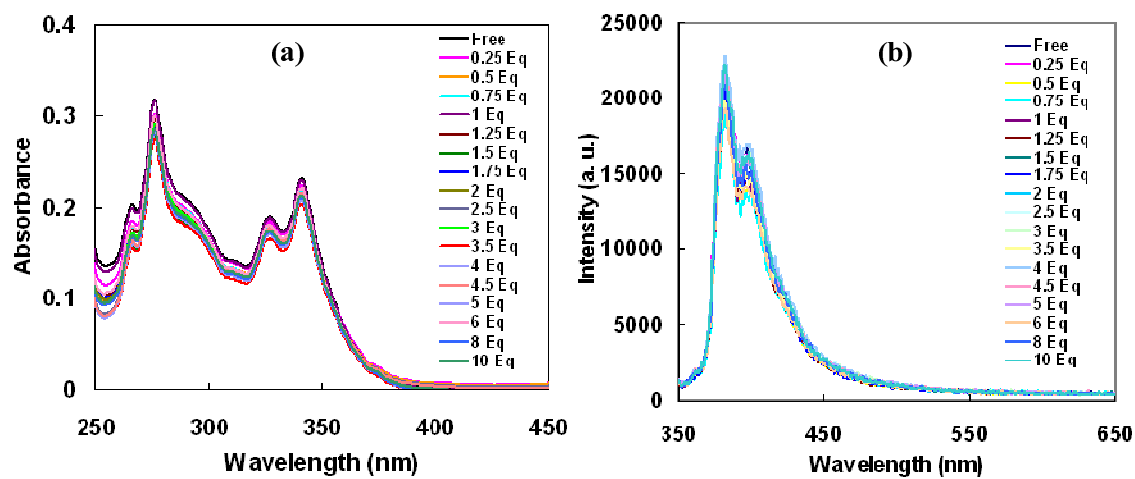


Figure S16: (a) UV-Vis, (b) emission spectra of **1** (10 μ M) in presence of Mg²⁺ ion.

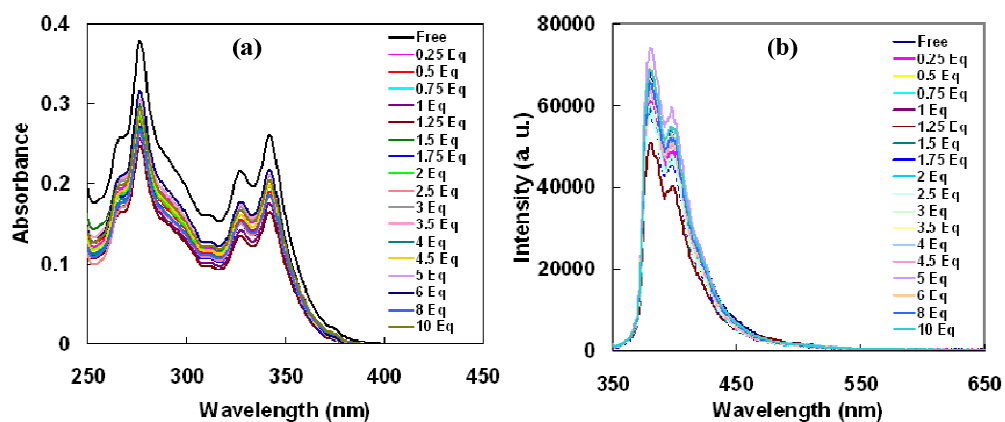


Figure S17: (a) UV-Vis, (b) emission spectra of **1** (10 μ M) in presence of Ca²⁺ ion.

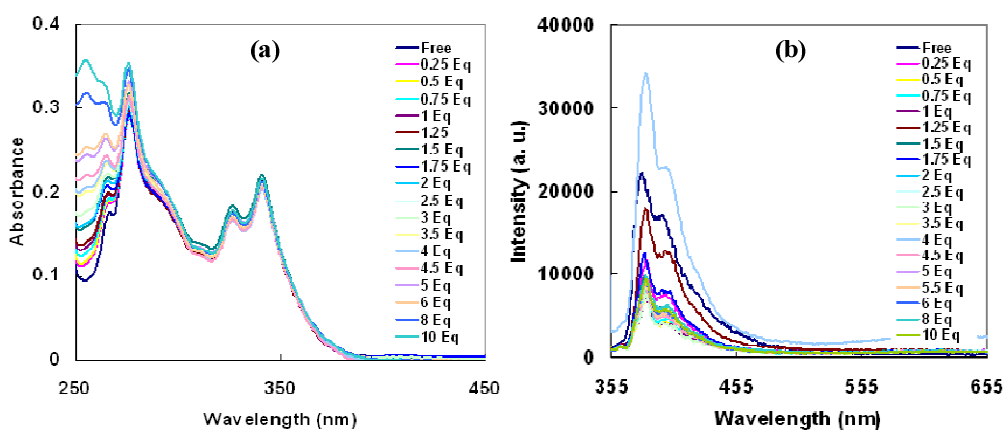


Figure S18: (a) UV-Vis, (b) emission spectra of **1** (10 μ M) in presence of Co²⁺ ion.

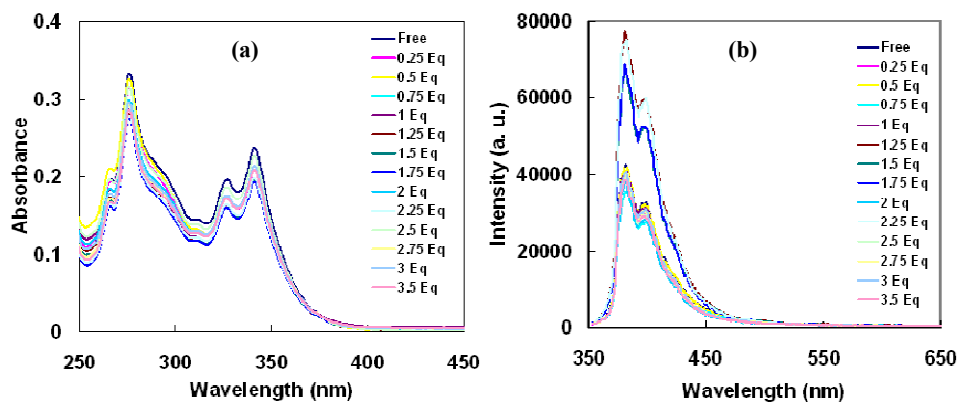


Figure S19: (a) UV-Vis, (b) emission spectra of **1** (10 μ M) in presence of Ni²⁺ ion.

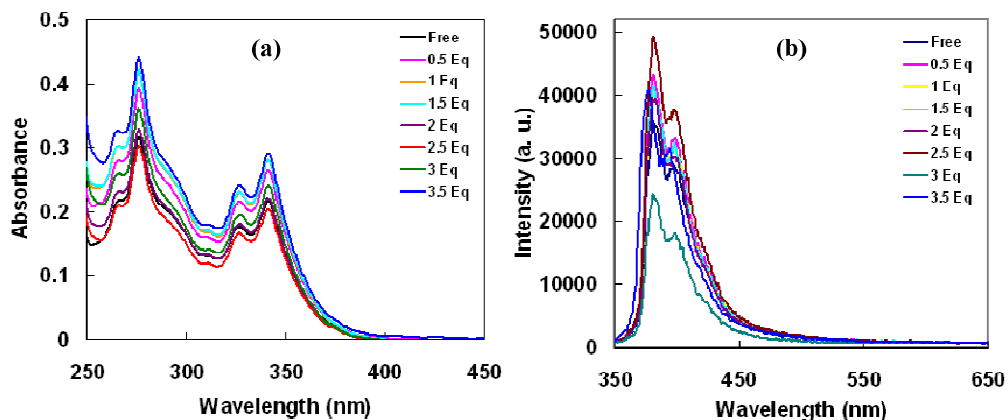


Figure S20: (a) UV-Vis, (b) emission spectra of **1** (10 μ M) in presence of Cu⁺ ion.

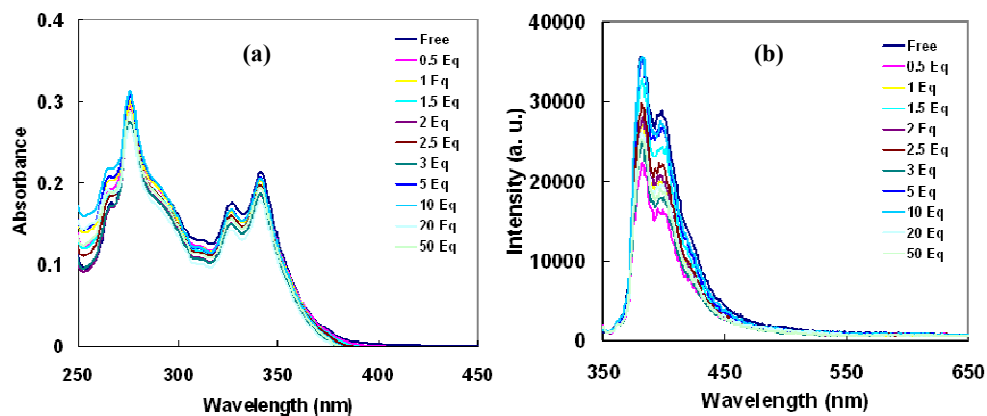


Figure S21: (a) UV-Vis, (b) emission spectra of **1** (10 μ M) in presence of Zn²⁺ ion.

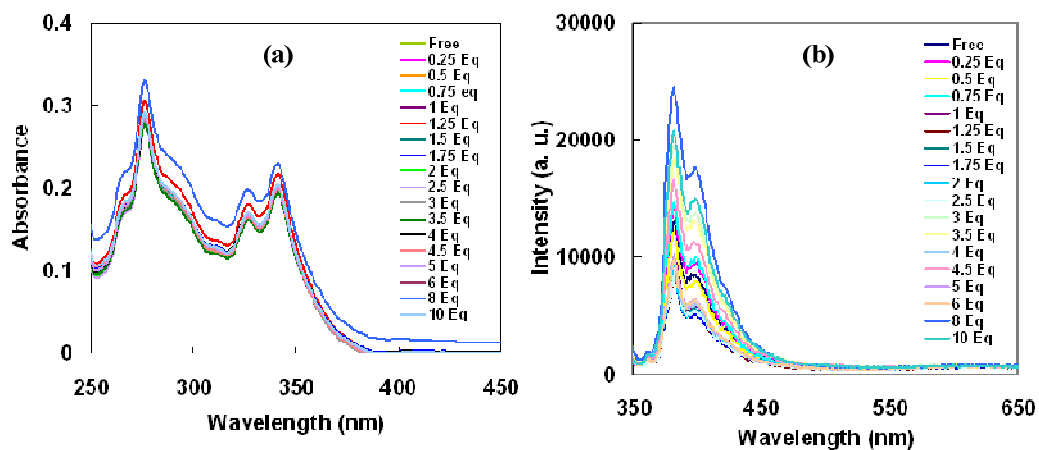


Figure S22: (a) UV-Vis, (b) emission spectra of **1** (10 μ M) in presence of Ag⁺ ion.

10. Comparison among the three fluorophores toward their efficiencies as selective fluorophores

The role of the donor dimethylamino phenyl substituent in selective sensing of Cu^{2+} was established by synthesizing other substituted phenyls, such as, fluorophore **2** ($^{\text{TCNP}}\text{Py}$) containing an electron withdrawing substituents (-CN) and **3** ($^{\text{TP}}\text{Py}$) with no substitution at phenyl ring and studied their specificity/selectivity in sensing the same metal ion. These two fluorophores show only a single emission band at around 380 nm which are characteristics of pyrene vibronic structures of the monomer emission both in presence or in absence of any metal ions in acetonitrile.

We have examined the optical sensor property of our probes **2-3** for metal ions, the tested metal Na^+ , Mg^{2+} , Ni^{2+} , and Cu^{2+} ions were added to the solution of **2-3**, respectively, and photophysical properties were studied. Thus, from the UV-visible absorption it was observed that the including Cu^{2+} ion no metal ions induced any change in absorption spectra, which implied that no metal ion interact significantly in a well-defined manner with both the probes **2-3** under the experimental condition.

The addition of various concentrations of metal ions including Cu^{2+} ion, only a single monomer emission with no significant change in fluorescence emission were observed (Figure S23 to Figure S30). However, in presence of large excess of Cu^{2+} ion ($>50 \mu\text{M}$), quenching of the monomer emission was observed. Therefore, from the metal titration experiments in presence and/or absence of Cu^{2+} ions and other metal ions, it was clear that both of the latter synthesized fluorophores (**2-3**) did not induce any selective change in absorbance or fluorescence intensity of the probes. Also in a competitive scenario, in presence of other background metal ions, addition of Cu^{2+} ions to any of the probe's solution does not bring any change in fluorescence intensity of the probes. This observation suggests that probes **2-3** are inefficient to interact significantly with any metal ions tested. These observations are totally opposite of that observed in case of probe **1** that showed a clear selectivity in sensing of Cu^{2+} ion. The results can easily be explained if we consider the probable role of donating and/or acceptor substituent. Thus, in case of probe **1** the donor *N,N*-dimethylaminophenyl group is donating the electron which is accumulated within the nitrogens of triazole ring yielding to better coordinating nitrogens for Cu^{2+} ions. However, in case of probe **2**, the acceptor unit (-CN) is withdrawing the electron density from the triazole's nitrogens, therefore, the less electron dense triazole's nitrogens are unable to coordinate with metal ions. In case of probe **3**, the intermediate situation, also we observed no interaction with metal ions. Therefore, it is clear that the presence of donor *N,N*-dimethylaminophenyl unit is mainly responsible for Cu^{2+} ion coordination and detection with high selectivity and large fluorescence enhancement.

10.1. UV-Vis and emission spectra of fluorophores 2-3 in presence of different metal ions

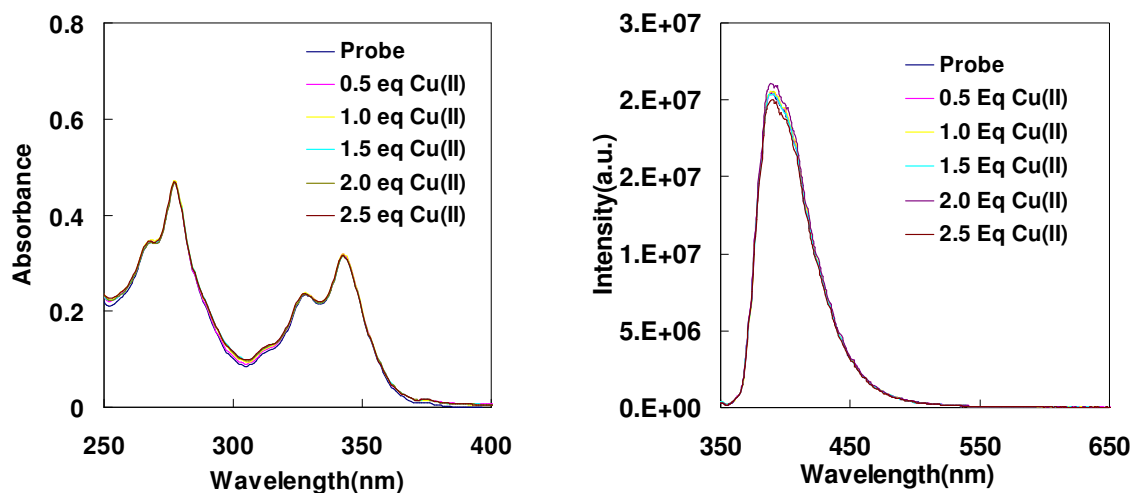


Figure S23: (a) UV-visible and (b) fluorescence spectra of 4-(1-(Pyren-1-yl)-1H-1,2,3-triazol-4-yl)benzotrile (**2**) in acetonitrile in presence of Cu^{2+} ion. [10 μM , r.t.; $\lambda_{\text{ex}} = 342$ nm].

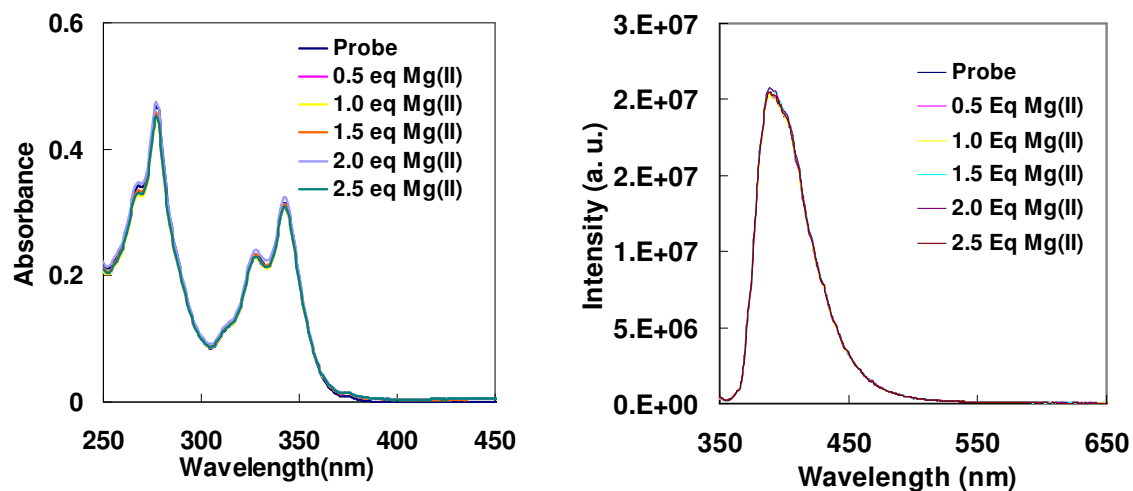


Figure S24: (a) UV-visible and (b) fluorescence spectra of 4-(1-(Pyren-1-yl)-1H-1,2,3-triazol-4-yl)benzotrile (**2**) in acetonitrile in presence of Mg^{2+} ion [10 μM , r.t.; $\lambda_{\text{ex}} = 342$ nm].

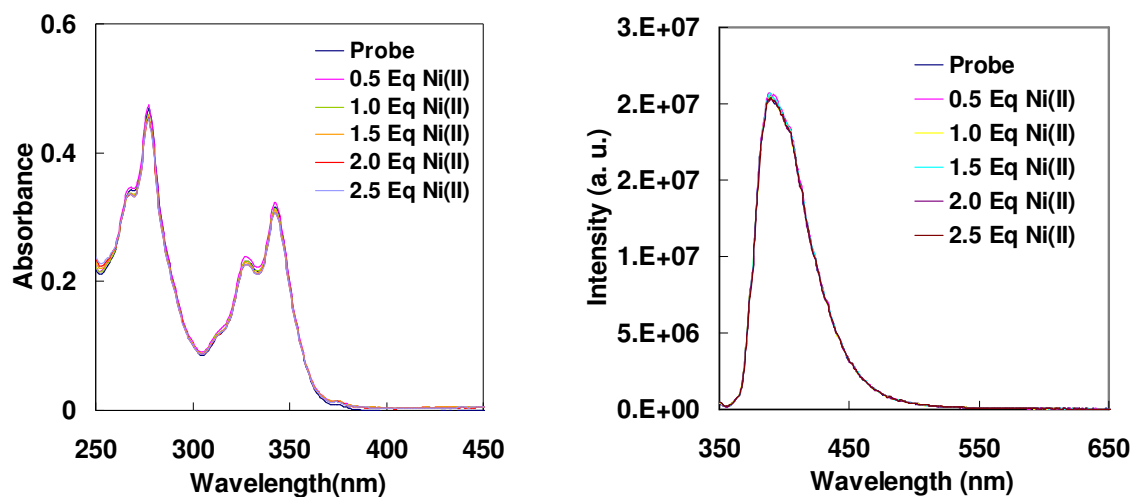


Figure S25: (a) UV-visible and (b) fluorescence spectra of 4-(1-(Pyren-1-yl)-1H-1,2,3-triazol-4-yl)benzotrile (**2**) in acetonitrile in presence of Ni²⁺ ion [10 μ M, r.t.; λ_{ex} = 342 nm].

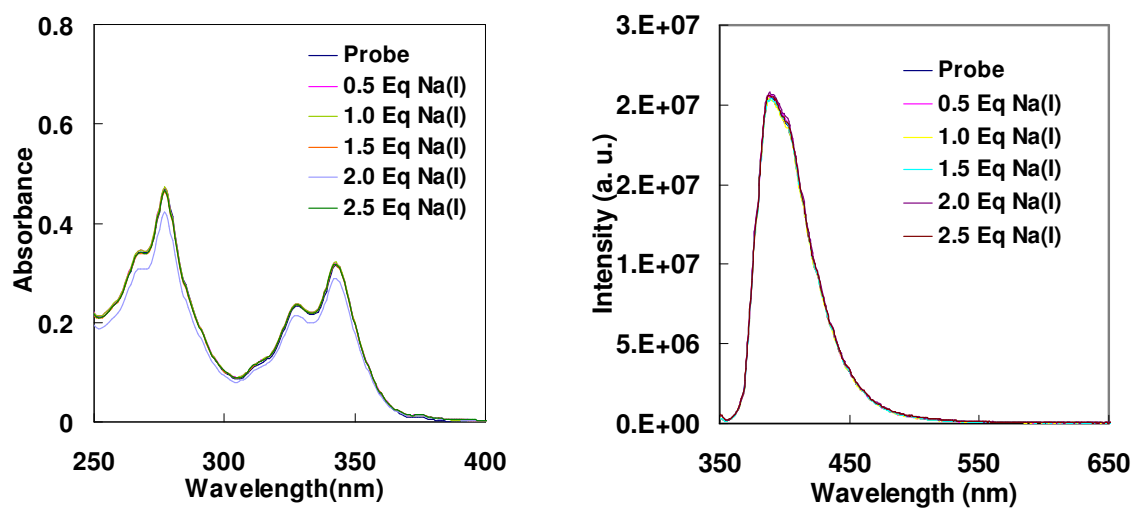


Figure S26: (a) UV-visible and (b) fluorescence spectra of 4-(1-(Pyren-1-yl)-1H-1,2,3-triazol-4-yl)benzotrile (**2**) in acetonitrile in presence of Na⁺ ion [10 μ M, r.t.; λ_{ex} = 342 nm].

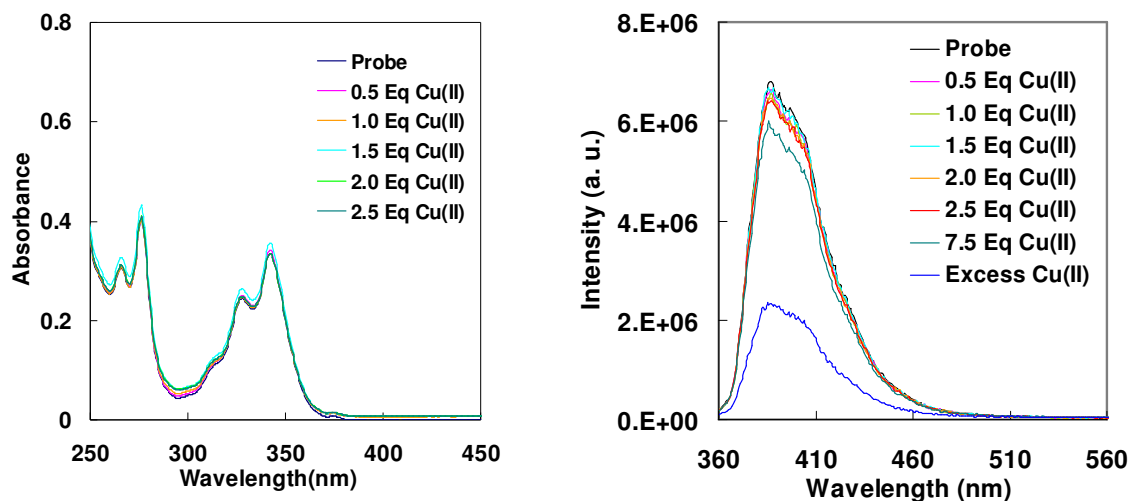


Figure S27: (a) UV-visible and (b) fluorescence spectra of 4-(1-(Pyren-1-yl)-1H-1,2,3-triazol-4-yl)benzene (**3**) in acetonitrile in presence of Cu^{2+} ion [$10 \mu\text{M}$, r.t.; $\lambda_{\text{ex}} = 342 \text{ nm}$].

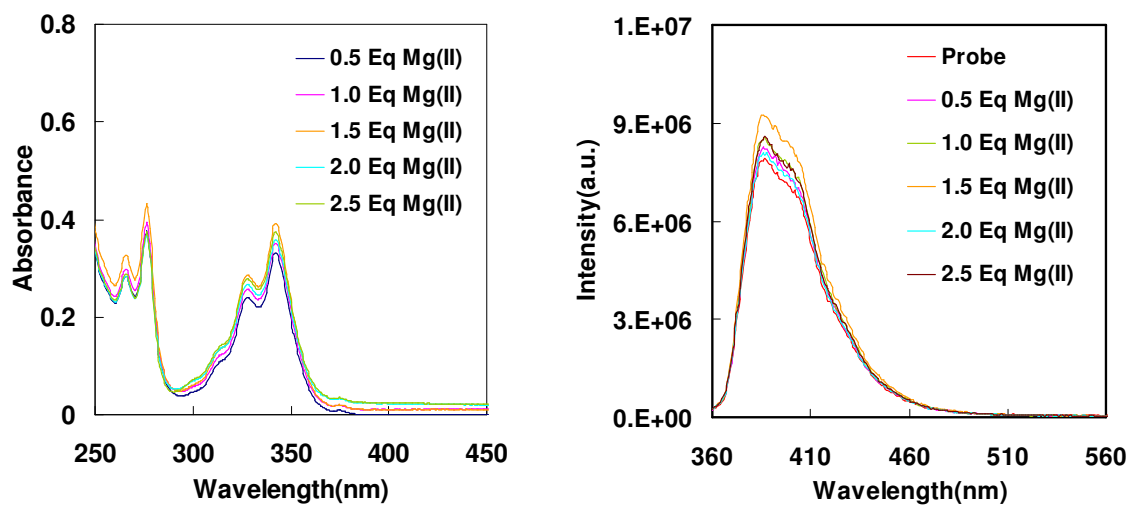


Figure S28: (a) UV-visible and (b) fluorescence spectra of 4-(1-(Pyren-1-yl)-1H-1,2,3-triazol-4-yl)benzene (**3**) in acetonitrile in presence of Mg^{2+} ion [$10 \mu\text{M}$, r.t.; $\lambda_{\text{ex}} = 342 \text{ nm}$].

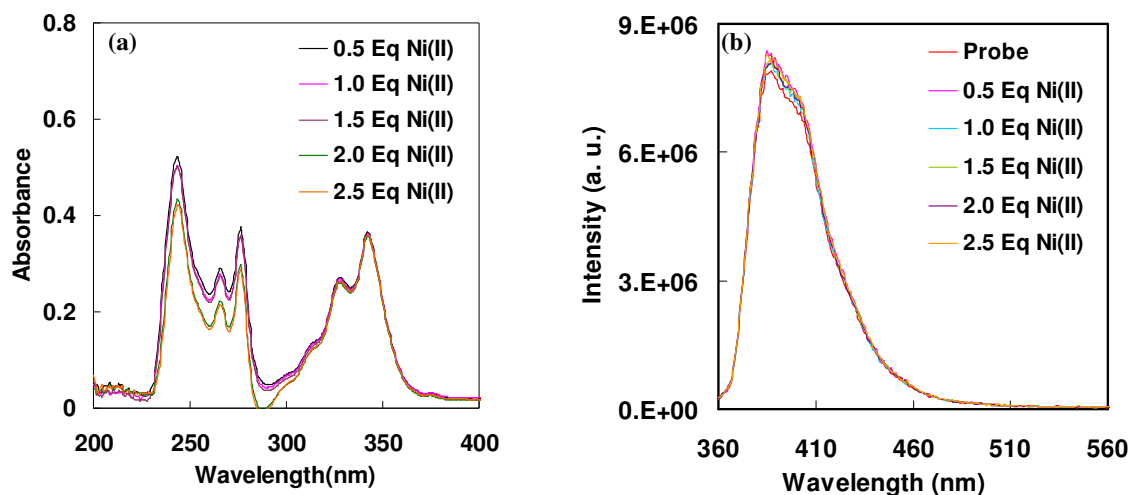


Figure S29: (a) UV-visible and (b) fluorescence spectra of 4-(1-(Pyren-1-yl)-1H-1,2,3-triazol-4-yl)benzene in acetonitrile in presence of Ni²⁺ ion [10 μM, r.t.; λ_{ex} = 342 nm].

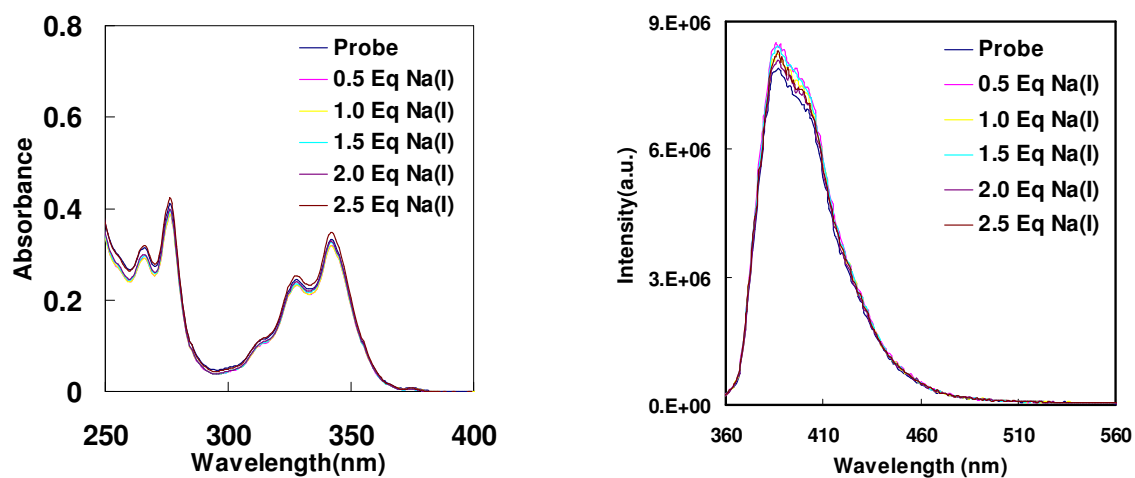


Figure S30: (a) UV-visible and (b) fluorescence spectra of 4-(1-(Pyren-1-yl)-1H-1,2,3-triazol-4-yl)benzene in acetonitrile in presence of Na⁺ ion [10 μM, r.t.; λ_{ex} = 342 nm].

10.2. Test for Selectivity in Sensing of Cu²⁺ Ion

Competition experiments were carried out to examine ion-selective fluorescence emission if all is shown by the fluorophores 2-3, though they did not show any specificity in sensing any of the metal ions tested. Thus, to do so, the fluorescence spectra (**Figure S31-32**) of the probe (10 μM) were taken in presence of Cu²⁺ ion (20 μM) along with other background metal ions in 50 equiv. excess concentration each. Although the fluorescence property of the probe with Cu²⁺ ion in presence of other background metal ions did not change. Thus, this result indicated that the probes are not all selective for Cu²⁺ or for any other metal ions tested.

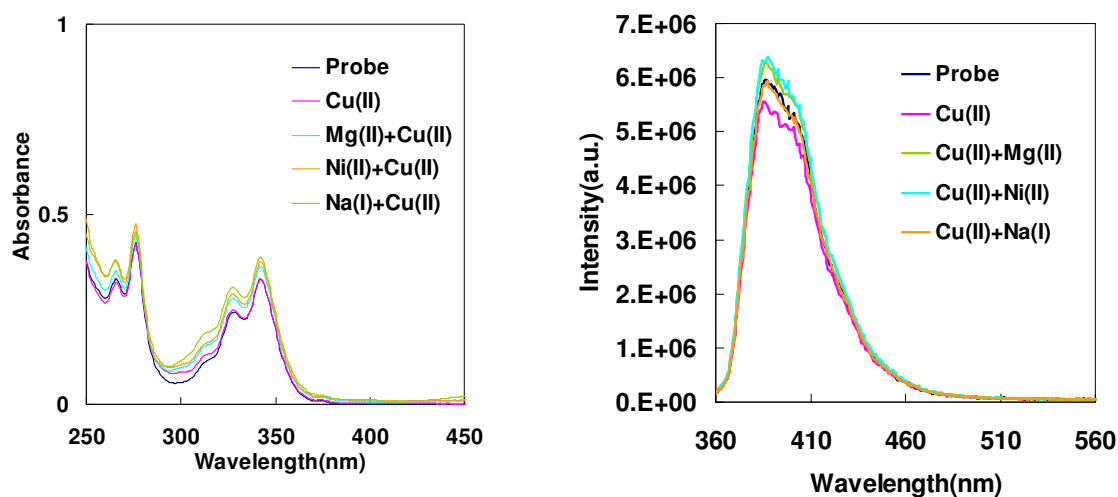


Figure S31a: (a) UV-visible and (b) fluorescence spectra ($\lambda_{\text{ex}} = 343 \text{ nm}$) of 4-(1-(Pyren-1-yl)-1H-1,2,3-triazol-4-yl)benzotrile (**2**) (10 μM) with Cu²⁺ ion (2 equiv.) in absence and presence of other metal ions (50 equiv.).

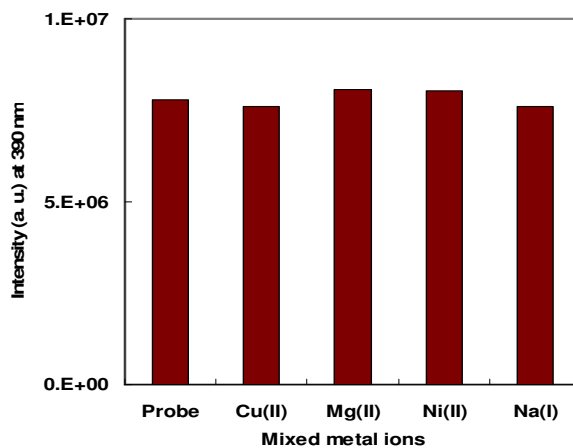


Figure S31b: Change in Fluorescence intensity at 390 nm (I_{390}) of 4-(1-(Pyren-1-yl)-1H-1,2,3-triazol-4-yl)benzotrile(10 μ M) with Cu^{2+} ion (2 equiv.) in absence and presence of other metal ions (50 equiv.).

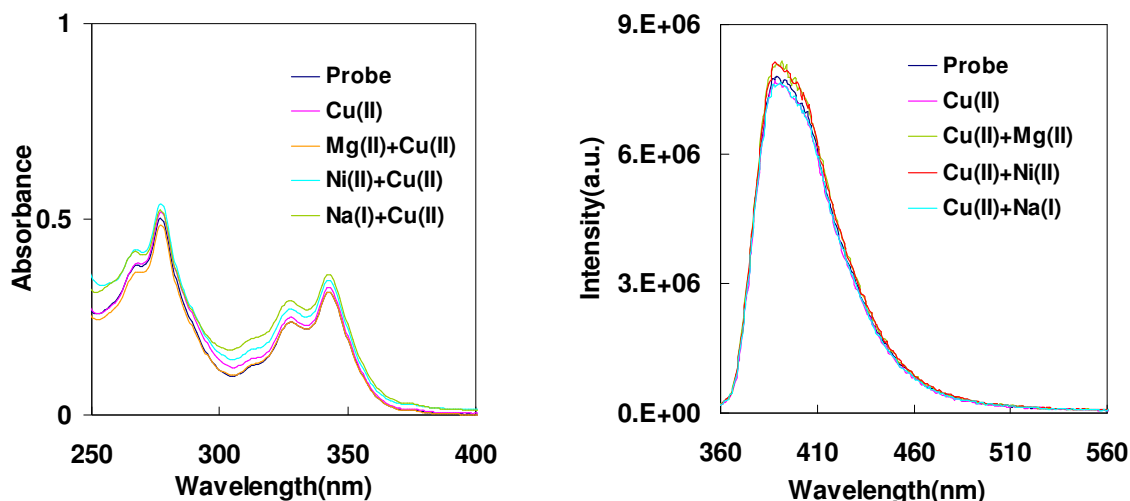


Figure S32a: (a) UV-visible and (b) fluorescence spectra ($\lambda_{\text{ex}} = 343$ nm) of 4-(1-(Pyren-1-yl)-1H-1,2,3-triazol-4-yl) benzene (**3**) (10 μ M) with Cu^{2+} ion (2 equiv.) in absence and presence of other metal ions (50 equiv.).

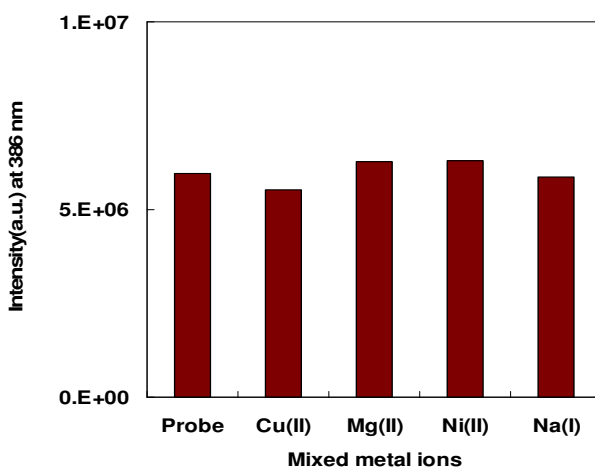


Figure 32b: Change in Fluorescence intensity at 386 nm (I_{386}) ratio of fluorescence intensity of 4-(1-(Pyren-1-yl)-1H-1,2,3-triazol-4-yl)benzene (10 μ M) with Cu^{2+} ion (2 equiv.) in absence and presence of other metal ions (50 equiv.).

11. Gaussian optimized geometry of 1-Cu²⁺ complex

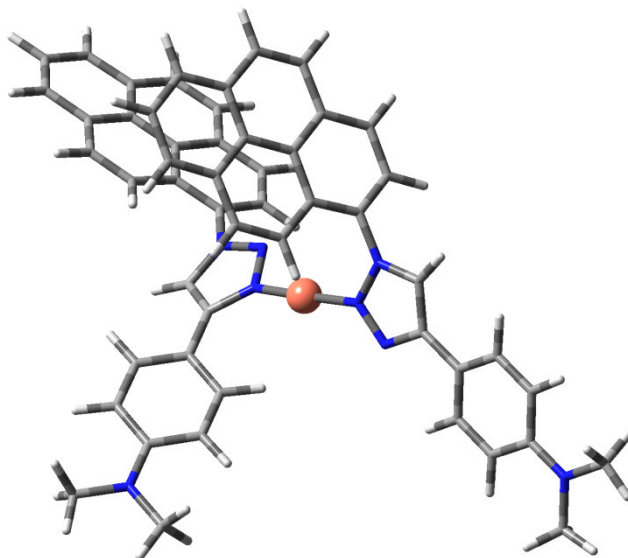


Figure S33: B3LYP/3-21G* energy minimized structure of **1.Cu²⁺** complex by DFT calculation. The LANL2DZ basis set was used for the Cu²⁺ cation.

Cartesian Co-ordinate:

$$E(\text{UB+HF-LYP}) = -2625.96196719 \text{ a.u.}$$

2	2		
N	0.56908000	1.14276400	-0.70243700
N	2.66532400	1.10615400	-1.30839800
N	1.47729900	0.37796800	-1.37849000
N	-1.50230000	6.44281900	2.60668200
C	3.82905600	0.62970800	-1.99517700
C	1.15404900	2.30480700	-0.22157800
C	0.45480900	3.34291200	0.51878200
C	2.48291100	2.27431700	-0.62126800
H	3.25828000	3.00971100	-0.51538500
C	5.08465400	0.58530400	-1.34433300
C	3.67825000	0.23139600	-3.32568200
H	2.69637200	0.27116800	-3.77731400
C	6.06290100	-0.20258100	-3.48941600
C	6.21852900	0.17727900	-2.11915400
C	7.51284000	0.14350900	-1.52042300
C	1.14499000	4.13776800	1.45729200
H	2.19131200	3.94101800	1.66099500

C	0.50877700	5.15023700	2.14737300
H	1.07481400	5.73032800	2.86120200
C	-1.56087600	4.62201900	0.98993400
H	-2.60471900	4.80605400	0.78183800
C	-0.91176200	3.61216000	0.30483000
H	-1.46100800	3.04775800	-0.44105300
C	-0.87092500	5.43310700	1.93571000
C	5.27847600	0.89187600	0.04523800
H	4.41951900	1.13437200	0.65723100
C	4.77631000	-0.18352400	-4.06289800
H	4.65082700	-0.47720400	-5.09793400
C	8.64952200	-0.24348900	-2.29483900
C	7.68008500	0.49213200	-0.14686100
C	9.91906400	-0.25986000	-1.68566600
H	10.78239700	-0.54882100	-2.27403100
C	8.46045700	-0.60699300	-3.66939200
H	9.32796300	-0.89971100	-4.24974000
C	6.51895700	0.84657200	0.61365400
H	6.64246200	1.07108400	1.66726000
C	10.07281100	0.08817500	-0.34421700
H	11.05730300	0.06889800	0.10599000
C	7.22051400	-0.59234300	-4.24089100
H	7.08984300	-0.87409700	-5.27910800
C	8.96854900	0.45739700	0.42107200
H	9.09421900	0.72136100	1.46498500
C	-2.93224800	6.72876600	2.36306200
H	-3.10489500	6.99374600	1.31346200
H	-3.23131100	7.57005400	2.98692500
H	-3.55386600	5.86353800	2.62140200
C	-0.76091600	7.28448300	3.57200300
H	-0.35440100	6.67700400	4.38858700
H	-1.44632300	8.01843500	3.99393600
H	0.06010200	7.81623000	3.07756500
N	-4.00631300	-0.03771700	-0.90068100
N	-3.01554500	-1.92142200	-0.22760000
N	-2.82041800	-0.55276500	-0.53667500
N	-10.36559500	-0.10542500	-2.20928000
C	-1.91466000	-2.76350900	0.15850700
C	-4.95192000	-1.04084400	-0.84141000
C	-6.34396000	-0.81530800	-1.18344800
C	-4.32140100	-2.21691500	-0.41673600
H	-4.71266200	-3.20038100	-0.23189800
C	-1.31770000	-2.58711200	1.42489200
C	-1.46760900	-3.73343000	-0.74344100
H	-1.94999100	-3.82753400	-1.70866800
C	0.23737300	-4.43370300	0.83909600

C	-0.21946800	-3.44076100	1.76350200
C	0.41237300	-3.31017400	3.03587000
C	-7.30848900	-1.84018200	-1.08641100
H	-7.02296100	-2.82771200	-0.74404800
C	-8.62759100	-1.61356100	-1.41918600
H	-9.33526400	-2.42442400	-1.33013600
C	-8.07849200	0.69526200	-1.96925900
H	-8.35934500	1.67998400	-2.31285600
C	-6.76390900	0.45572000	-1.63153500
H	-6.03169200	1.24849500	-1.71321000
C	-9.06219400	-0.33386200	-1.87537300
C	-1.77063600	-1.62034400	2.39038400
H	-2.62035800	-0.99435200	2.14880700
C	-0.40551200	-4.56067000	-0.40656200
H	-0.06255100	-5.31089600	-1.10856300
C	1.50287000	-4.16543100	3.38252300
C	-0.04877800	-2.33494700	3.97210200
C	2.10403400	-4.02632000	4.64506300
H	2.92816100	-4.67785600	4.91231700
C	1.94224000	-5.14810600	2.42874200
H	2.76843000	-5.79488900	2.70166900
C	-1.16001200	-1.50314500	3.60371800
H	-1.52085000	-0.77918100	4.32620500
C	1.64673200	-3.07082500	5.55239600
H	2.11863800	-2.98426700	6.52327300
C	1.33872500	-5.27746800	1.21476300
H	1.67607600	-6.02667500	0.50811900
C	0.58241600	-2.23292300	5.22365300
H	0.22735000	-1.49881300	5.93810400
C	-10.80216800	1.22782700	-2.68774500
H	-10.61458100	1.99188000	-1.92555400
H	-11.87094400	1.19236000	-2.89246500
H	-10.27540900	1.49875300	-3.60924800
C	-11.37561200	-1.18616800	-2.10850600
H	-11.11333900	-2.02262000	-2.76543300
H	-12.34236800	-0.79005400	-2.41497800
H	-11.45375700	-1.54651300	-1.07704800
Cu	-1.13209600	0.31647400	-0.54791700